Inactivation of HNSCC Cells by ^{90}Y-Labeled Cetuximab Strictly Depends on the Number of Induced DNA Double-Strand Breaks

Jarob Saker[1], Malte Kriegs[1], Martin Zenker[2], Jan-Martin Heldt[2], Iris Eke[3], Hans-Jürgen Pietzsch[2], Reidar Grénman[4], Nils Cordes[3,5], Cordula Petersen[6], Michael Baumann[3,5], Jörg Steinbach[2], Ekkehard Dikomey[1], and Ulla Kasten-Pisula[1]

[1]Laboratory of Radiobiology and Experimental Radiooncology, University Medical Centre Hamburg-Eppendorf/Hubertus Wald Cancer Centre, Hamburg, Germany; [2]Institute for Radiopharmacy, Helmholtz-Zentrum Dresden-Rossendorf, Dresden, Germany; [3]OncoRay National Center for Radiation Research in Oncology, Technical University Dresden, Dresden, Germany; [4]Departments of Otorhinolaryngology–Head and Neck Surgery and Medical Biochemistry and Genetics, Turku University and University Hospital of Turku, Turku, Finland; [5]Department of Radiation Oncology, Hospital Carl Gustav Carus, Technical University Dresden, Dresden, Germany; and [6]Clinic for Radiotherapy and Radiooncology, University Medical Centre Hamburg-Eppendorf/Hubertus Wald Cancer Centre, Hamburg, Germany

Radioimmunotherapy is considered to have great potential for efficient and highly specific treatment of tumors. The aim of this study was to determine the efficacy of radioimmunotherapy when using ^{90}Y-labeled cetuximab and to determine to what degree induction and repair of DNA double-strand breaks (DSBs) are decisive for this approach. **Methods:** This study was performed with 9 cell lines of squamous cell carcinoma of the head and neck (HNSCC) differing strongly in epidermal growth factor receptor (EGFR) expression. The radionuclide ^{90}Y was coupled by the chelator *trans*-cyclohexyl-diethylene-triamine-pentaacetic acid (CHX-A″-DTPA)/linker construct to the EGFR-directed antibody cetuximab to yield ^{90}Y-Y-CHX-A″-DTPA-cetuximab with a specific activity of approximately 1.2 GBq/mg. EGFR expression was determined by immunofluorescence and Western blotting, cetuximab binding by fluorescence-activated cell sorter analysis, the number of DSBs by immunofluorescence staining γH2AX/53BP1-positive repair foci, and cell survival by colony formation. **Results:** For the 9 HNSCC cell lines, cetuximab binding correlated with the amount of EGFR present in the cell membrane ($r^2 = 0.967$, $P < 0.001$). When cells were exposed to ^{90}Y-Y-CHX-A″-DTPA-cetuximab, the number of induced DSBs increased linearly with time ($r^2 = 0.968$, $P = 0.016$). This number was found to correlate with the amount of membranous EGFR ($r^2 = 0.877$, $P = 0.006$). Most DSBs were repaired during incubation at 37°C, but the small number of remaining DSBs still correlated with the amount of membranous EGFR (24 h: $r^2 = 0.977$, $P < 0.001$; 48 h: $r^2 = 0.947$, $P < 0.001$). Exposure to ^{90}Y-Y-CHX-A″-DTPA-cetuximab also resulted in efficient cell killing, whereby the extent of cell killing correlated strongly with the respective number of remaining DSBs ($r^2 = 0.989$, $P < 0.001$) and with the amount of membranous EGFR ($r^2 = 0.967$, $P < 0.001$). No cell killing was observed for UTSCC15 cells with low EGFR expression, in contrast to the strong reduction of 86% measured for UTSCC14 cells showing a strong overexpression of EGFR. **Conclusion:** ^{90}Y-Y-CHX-A″-DTPA-cetuximab affected cell survival through the induction of DSBs. This treatment was especially efficient for HNSCC cells strongly overexpressing EGFR, whereas no effect was seen for cells with low levels of EGFR expression. Therefore, EGFR-directed radioimmunotherapy using ^{90}Y-Y-CHX-A″-DTPA-cetuximab appears to be a powerful tool that can be used to inactivate tumors with strong EGFR overexpression, which are often characterized by a pronounced radioresistance.

Key Words: targeted radioimmunotherapy; EGFR; ^{90}Y-Y-CHX-A″-DTPA-cetuximab; double-strand breaks; cell inactivation

J Nucl Med 2013; 54:416–423
DOI: 10.2967/jnumed.111.101857

External-beam radiotherapy is a major pillar of cancer treatment. Although significant progress has been made in the planning and application of external-beam radiotherapy in recent years, there is still a significant proportion of tumors for which the dose that carries an acceptable risk of normal-tissue damage is not high enough for local control. One concept that might tackle this problem is to deliver an additional dose by systemic approaches specifically to the tumor. Such delivery can be achieved by radiolabeled monoclonal antibodies (mAbs), provided that the epitope recognized by the mAb will allow for the specific targeting of tumor cells.

In this context, the epidermal growth factor receptor (EGFR) is of great interest. Its expression in normal tissue is relatively low, compared with the high expression often found in tumors, especially those of epidermal origin such as squamous cell carcinoma of the head and neck (HNSCC) (*1,2*). Beyond that, the overexpression of EGFR is also associated with a more aggressive tumor phenotype featuring

Received Dec. 13, 2011; revision accepted Oct. 3, 2012.
For correspondence contact: Ekkehard Dikomey, Laboratory of Radiobiology and Experimental Radiooncology, University Medical Centre Hamburg-Eppendorf, Martinistrasse 52, 20246 Hamburg, Germany.
E-mail: dikomey@uke.de
Published online Jan. 23, 2013.

increased radio- and chemoresistance, resulting in a poor prognosis (*3*). Consequently, there is great need to develop new and more efficient therapies, especially for HNSCC tumors overexpressing EGFR (*4,5*).

Current EGFR-targeting strategies aim primarily at radiosensitization through the blockade of EGFR-dependent signaling pathways using either mAbs (e.g., cetuximab) or tyrosine kinase inhibitors (e.g., gefitinib) (*4*). Bonner et al. (*6*) have shown their clinical relevance for advanced HNSCC when combined with radiotherapy. However, that study and preclinical studies (*7*) have also revealed that only a subgroup of HNSCC patients may actually benefit from this new approach.

Alternatively, EGFR may also serve as a target for radioimmunotherapy by using radiolabeled EGFR-directed mAbs. Several preclinical studies using xenografts have already demonstrated that such an EGFR-directed therapy can result in efficient treatment (*8–13*). The outcome of this treatment was shown to depend on the amount of radiolabeled mAb ultimately concentrated in the tumor. This amount, in turn, depends not only on the level of EGFR expression but also on the vascular architecture of the specific tumor (*8,9,11,14*).

So far, the effect of radiolabeled EGFR-directed mAbs on tumor growth has been attributed to their antiangiogenic effects and to increased apoptosis (*8*). The aim of our study was to determine the extent to which these effects may also depend on the number of DNA double-strand breaks (DSB) induced by the radiolabeled mAb bound to the cell. DSBs constitute the most critical form of DNA damage induced by ionizing irradiation, with even a small fraction of residual DSBs having a great impact on cell survival (*15,16*). This study, conducted as part of a German consortium investigating the combination of external-beam radiotherapy with radioimmunotherapy, was performed on 9 HNSCC cell lines differing strongly in EGFR expression (*2*). Cells were exposed to cetuximab labeled with ^{90}Y via the chelator *trans*-cyclohexyl-diethylene-triamine-pentaacetic acid (CHX-A″-DTPA) with a specific activity of about 1.2 GBq/mg. Induction and repair of DSBs were determined by immunostaining of γH2AX/53BP1-positive repair foci and cell survival by colony assay.

MATERIALS AND METHODS

Preparation of Cetuximab Conjugates

Preparation of radiolabeled cetuximab conjugates will be described in detail in another publication by our group. Briefly, before protein conjugation, CHX-A″-DTPA was dissolved in *N*-(2-hydroxyethyl)piperazine-*N*′-(2-ethanesulfonic acid) buffer (400 μL, 500 mM, pH 7.2) and added to the cetuximab solution to achieve a molar ratio of 20:1 (CHX-A″-DTPA:cetuximab). The mixture was allowed to react for 24 h at 25°C without stirring. Excess CHX-A″-DTPA was removed by a Jumbosep 30-kDa molecular-weight-cutoff concentrator (Pall Life Sciences). The buffer change was performed with an NH_4OAc solution (50 mM, pH 6.0) containing NaCl (150 mM).

For the radiolabeling of CHX-A″-DTPA-cetuximab with ^{90}Y, a solution of ^{90}Y-YCl_3 (Yttriga; Eckert and Ziegler Nuclitec GmbH) in HCl (0.04 M, 120 MBq) was added to the antibody conjugate (100 μg) plus MES buffer (100 μL, 200 mM, pH 6.1), immediately stirred with a vortex mixer, and incubated for 30 min at 30°C without shaking. To quench the labeling reaction and fix nonreacted radionuclides, free DTPA chelator (32 μL, 0.1 μg/μL) was added to the reaction mixture. Radiochemical yield was determined by radio–instant thin-layer chromatography; a 10-cm silicic-acid strip (Varian GmbH) was used as the stationary phase, and a 0.9% NaCl solution was used as the mobile phase. The radiolabeled antibody was purified by spin filtration using a 30-kDa Microcon device (Millipore). The obtained ^{90}Y-Y-CHX-A″-DTPA-cetuximab was always synthesized to have a specific activity of 1.2 GBq/mg.

Cell Cultures

Experiments were performed with head and neck squamous cell carcinoma (HNSCC) cell lines Cal33, FaDuDD, HSC4, SAS, SAT, XF354, UTSCC5, UTSCC14, and UTSCC15, as well as the epithelial carcinoma cell line A431. All cell lines were grown in Dulbecco modified Eagle medium (Gibco) containing 10% fetal bovine serum (Biochrom AG) and 4 mM glutamine (Gibco) at 37°C, 10% CO_2, and 100% humidification. Cells were routinely screened for *Mycoplasma* infection.

X-Irradiation

Cells were irradiated at room temperature with 200-kV x-rays (RS225 [Gulmay Medical Ltd.], 15 mA, 0.8-mm beryllium and 0.5-mm copper filtering, dose rate of 1.2 Gy/min).

Small Interfering RNA (siRNA) Transfection

EGFR was downregulated via siRNA. To this end, 1.2×10^6 cells were seeded in 10-cm plates 24 h before siRNA transfection; 20 nM anti-EGFR siRNA (5′-GGCACGAGUAACAAGCUCAtt-3′; Ambion) or control siRNA (5′-GCAGCUAUAUGAAUGUUGUtt-3′; MWG) was transfected using oligofectamine (Invitrogen) according to the manufacturer's instructions under serum-free conditions for 8 h. After 48 h of knockdown, cells were treated with ^{90}Y-Y-CHX-A″-DTPA-cetuximab or DTPA-cetuximab. Twenty-four hours later, cells were fixed for further analysis. The effect of knockdown was controlled by analysis of whole-cell lysates 48 h after transfection using Western blot.

Protein Isolation and Western Blot

Fractionated cell extracts were prepared as described previously (*2*). Briefly, cells were detached by scraping and were lysed by ultrasonic treatment, followed by ultracentrifugation (supernatant = cytoplasm). Pellets were resuspended in TritonX-100 buffer including protease inhibitors (Roche). The membranous fraction was achieved by centrifugation (supernatant). The remaining pellets (nuclei) were washed with TritonX-100 buffer and were resuspended into sample buffer.

Proteins were detected by Western blot according to standard protocols. The primary antibodies were anti-Calnexin (BD Pharmingen, 610523), anti-Calpain-1/2 small subunit (Callbiochem, 208730), anti-EGF receptor (Cell Signaling Technology, 2232), and anti-Histone 2B (Imgenix, IMG-359). Secondary antibodies were from GE Healthcare: antirabbit and antimouse HRP-conjugated NA934V and NA931V. Signals were determined via chemiluminescence using ECLTM Western blotting detection reagents (Amersham) and a light-sensitive camera system (Berthold).

Fluorescence-Activated Cell Sorter (FACS) Analysis

Cetuximab-binding capacity was determined according to the method of Diaz et al. (*17*) using fluorescein isothiocyanate–conjugated

antihuman IgG (H+L) (Dianova, 709-096-149). Briefly, individual living cells were incubated at 4°C with phosphate-buffered saline containing 30 nM cetuximab, washed, incubated with fluorescence-labeled secondary antibody, washed again, and then used for FACS analysis. FACS analysis was performed using the FACS Canto System and FACS Diva software (BD Biosciences).

Immunofluorescence

Immunofluorescent staining was performed as described previously (*18*). Briefly, cells were fixed, permeabilized, blocked with BSA, incubated with primary antibody, washed, and incubated with secondary antibody. After 4,6-diamino-2-phenylindole (QBiogene) staining and washing, cells were mounted in antifade mounting solution (QBiogene) and analyzed using a fluorescence microscope (Axioplan 2 [Zeiss], ×630 magnification).

Detection of Cetuximab Binding to EGFR. To determine the binding of cetuximab to EGFR, 30 nM cetuximab was used as the primary antibody and fluorescein isothiocyanate–conjugated antihuman IgG (H+L) (Dianov, 709-096-149) as the secondary antibody.

Detection of DNA Double-Strand Breaks. For costaining of γH2AX and 53BP1, antiphospho-Histone 2A.x (Ser139; Millipore, 05-636) and anti-53BP1 (Novus Biologicals, NB100-305) were used as primary antibodies. Secondary antibodies included antimouse ALEXA fluor594 (Molecular Probes, A11005) and antirabbit Fluorescein (GE Healthcare, N1034). Two hundred randomly chosen intact nuclei were analyzed per treatment group. 53BP1- and γH2AX-positive foci were counted visually using the fluorescence microscope. For these experiments, cells were plated on 12-well plates, with the number of cells seeded per plate depending on time exposed to ^{90}Y-Y-CHX-A″-DTPA-cetuximab (<24 h, n = 150,000; 24 h, n = 100,000; 48 h, n = 50,000). The number of foci counted in cells treated with CHX-A″-DTPA-cetuximab was subtracted from that determined in cells treated with ^{90}Y-Y-CHX-A″-DTPA-cetuximab and was normalized to the DNA content of the respective cell line.

Cell Survival

Cells were treated with CHX-A″-DTPA-cetuximab/^{90}Y-Y-CHX-A″-DTPA-cetuximab as described above and incubated at 37°C for 48 h. Afterward, cells were trypsinized and seeded for colony formation assay at a concentration adjusted to the specific cellular plating efficiency. Culture flasks were fixed and stained 2 wk after seeding or when the colonies had grown to at least 50 cells.

Statistics

Data analysis and statistical evaluation were performed using Prism, version 4.03 (GraphPad Software). Values are expressed as means ± SEM. All experiments were repeated at least 3 times. The unpaired Student t test was performed in the statistical analysis. P values were calculated using 1-sided tests.

RESULTS

EGFR Heterogeneity and Cetuximab-Binding Capacity

The aim of this study was to characterize the efficiency and cellular mechanisms of radioimmunotherapy using ^{90}Y-labeled cetuximab.

The membranous EGFR expression varies remarkably throughout the different HNSCC cell lines, as shown by Western blot analysis of the fractionated cell extracts (Fig. 1A; Supplemental Fig. 1 [supplemental materials are available online only at http://jnm.snmjournals.org]). The binding of cetuximab to tumor cells depends on the amount of this EGFR fraction, as shown after 30 min of incubation by immunofluorescence (Fig. 1B). Quantifying the amount of EGFR-bound cetuximab by flow cytometry, we were able to show a strong linear correlation (r^2 = 0.967, $P < 0.001$) between the amount of cetuximab bound to the cell and the amount of EGFR expressed in the membrane (Fig. 1C).

Using the number of EGFR molecules previously determined for A431 cells by binding assay as a reference (*19*), we estimated the respective number present in the cell membrane of each cell line. These numbers varied from 2.4×10^5 molecules for UTSCC15 cells up to the 10-fold higher value of 3.12×10^6 molecules for UTSCC14 cells, reflecting the tremendous heterogeneity of EGFR expression observed in HNSCC.

Kinetics of DSB Induction and Repair

We next analyzed the induction of DNA damage by bound ^{90}Y-Y-CHX-A″-DTPA-cetuximab. To quantify DNA damage, we scored DSBs through the colocalization of γH2AX and 53BP1 foci (Fig. 2A). Both UTSCC14 and UTSCC15 cells were labeled with ^{90}Y-Y-CHX-A″-DTPA-

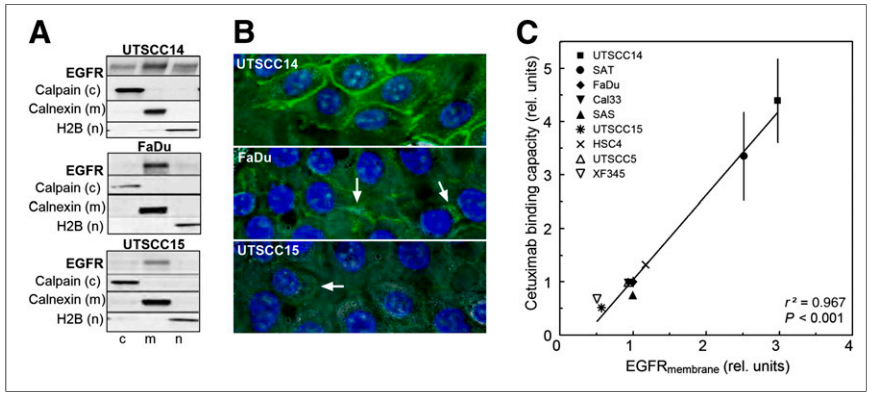

FIGURE 1. EGFR expression and cetuximab binding in HNSCC cell lines. (A) Expression of EGFR in cytoplasmatic (c), membranous (m), and nuclear (n) compartments as determined by Western blot. Specific marker proteins are used for quality control. (B) Detection of cetuximab bound to EGFR after incubation with 30 nM cetuximab for 30 min in UTSCC14, FaDu, and UTSCC15 cells by immunofluorescence staining. (C) Correlation between cetuximab binding capacity and relative amount of membranous EGFR. Amount of EGFR from 50,000 cells was quantified via Western blot, and cetuximab binding was measured by FACS analysis after incubation of living cells with 30 nM cetuximab at 4°C. Relative values are obtained after normalization to values obtained for FaDu cells.

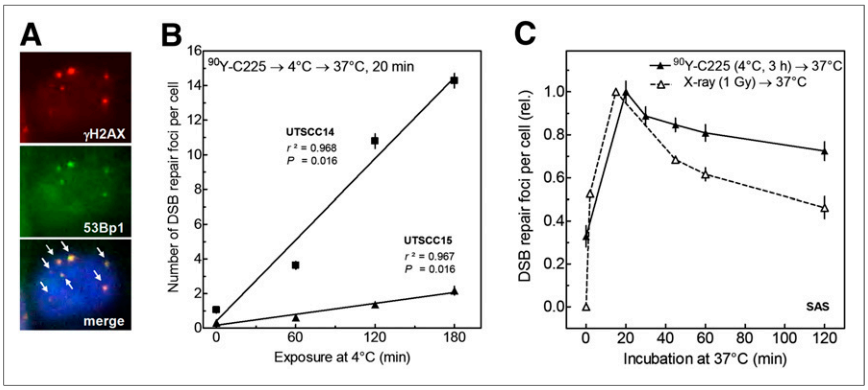

FIGURE 2. Induction and repair of DNA DSBs by ^{90}Y-Y-CHX-A″-DTPA-cetuximab. (A) Detection of DSBs by immunofluorescence staining of γH2AX/53BP1 foci. (B) Induction of DSBs by ^{90}Y-Y-CHX-A″-DTPA-cetuximab. UTSCC15 and UTSCC14 cells were incubated at 37°C for 5 min with 30 nM ^{90}Y-Y-CHX-A″-DTPA-cetuximab before being washed and incubated at 4°C for up to 3 h, followed by incubation at 37°C for 20 min to allow for focus formation. Data were fitted by linear regression. (C) Repair of DSBs. SAS cells were incubated for 5 min at 37°C with 30 nM ^{90}Y-Y-CHX-A″-DTPA-cetuximab before being washed and incubated at 4°C for 3 h (solid line), followed by incubation at 37°C for up to 120 min. Cells were irradiated with 1 Gy for sake of comparison. DSBs were detected via γH2AX/53BP1 focus formation. Number of DSBs detected was normalized to maximal number of DSBs scored.

cetuximab for 5 min, which was sufficient for complete binding (Supplemental Fig. 2). Cells were then washed and kept in drug-free medium at 4°C for up to 3 h, followed by an incubation at 37°C for 20 min to allow formation of DSB repair foci (Fig. 2A). For both cell lines, there was a linear increase in the number of DSBs throughout the incubation at 4°C (Fig. 2B).

We also analyzed the repair kinetics of DSB induced by bound ^{90}Y-Y-CHX-A″-DTPA-cetuximab (Fig. 2C). SAS cells were labeled with ^{90}Y-Y-CHX-A″-DTPA-cetuximab for 5 min, washed, and stored at 4°C for 3 h before being incubated at 37°C for up to 120 min. The number of DSB repair foci showed a peak after 20 min, followed by a continuous decline. These kinetics are similar to those measured after external x-irradiation with 1 Gy (Fig. 2C, open triangles). However, the decline in repair foci was less sharp after exposure to ^{90}Y-Y-CHX-A″-DTPA-cetuximab, because the number of repair foci measured there was determined both by repair and by induction of new foci resulting from new DSBs induced by ^{90}Y-Y-CHX-A″-DTPA-cetuximab.

Variation of Initial and Accumulated DSBs

The amount of EGFR present in the membrane fraction determined the number of DSBs induced when cells were exposed to bound ^{90}Y-Y-CHX-A″-DTPA-cetuximab at 4°C for 3 h (Fig. 3A). For 6 HNSCC cell lines differing markedly in EGFR surface expression, there was a linear correlation between the number of DSBs induced and the respective EGFR membrane fraction ($r^2 = 0.877$, $P = 0.005$). The larger the amount of membranous EGFR, the greater the number of DSBs induced during this incubation. The lowest rate of induction was measured for UTSCC15 cells, at 0.23 DSBs per hour, and the highest for UTSCC14 cells, at 4.61 DSBs per hour.

In Figure 3B, DSB induction by ^{90}Y-Y-CHX-A″-DTPA-cetuximab as measured for UTSCC15, FaDu, and UTSCC14 cells is compared with the induction of DSBs determined after x-ray exposure with 1 Gy. For x-irradiation, there was only a marginal variation in the number of DSBs induced, with an average of 36 DSBs per gray. In contrast, on exposure to ^{90}Y-Y-CHX-A″-DTPA-cetuximab for 3 h, the number of DSBs induced varied by a factor of almost 20. The number of DSBs measured in UTSCC15 cells after being exposed to ^{90}Y-Y-CHX-A″-DTPA-cetuximab for 3 h was equivalent to an x-ray dose of 0.02 Gy. Equivalent x-ray doses for FaDu and for UTSCC14 were 0.1 and 0.4 Gy, respectively. These data demonstrate that treatment with ^{90}Y-Y-CHX-A″-DTPA-cetuximab allows for the selective targeting of HNSCC cells with strong EGFR expression.

We also measured the number of DSBs remaining after longer repair intervals, since this number is known to essentially determine the extent of cell killing ultimately achieved (*16*). For these experiments, HNSCC cell lines were allowed to bind ^{90}Y-Y-CHX-A″-DTPA-cetuximab for 5 min before being incubated at 37°C for either 24 or 48 h. Figure 3C shows that after longer repair intervals, there were still a small number of remaining DSB repair foci, which correlated significantly with the amount of membranous EGFR (24 h: $r^2 = 0.977$, $P < 0.001$; 48 h: $r^2 = 0.947$, $P = 0.001$). The number of DSB repair foci present after 48 h was slightly lower than that after 24 h, because on the one hand there was more time to repair and on the other hand fewer DSBs were induced during the second half of the exposure time, as ^{90}Y decays with a half-life of 2.6 d. Most notably, these data demonstrate that even after longer repair periods, the number of remaining DSB repair foci is primarily determined by the amount of membranous EGFR, which in turn strictly depends on the amount of bound ^{90}Y-Y-CHX-A″-DTPA-cetuximab.

For UTSCC14 cells, we also determined that the induction of DSBs of ^{90}Y-Y-CHX-A″-DTPA-cetuximab specifically depends on EGFR. To this end, EGFR was downregulated by siRNA (inset of Fig. 3D). When normal UTSCC14 cells were exposed to bound ^{90}Y-Y-CHX-A″-

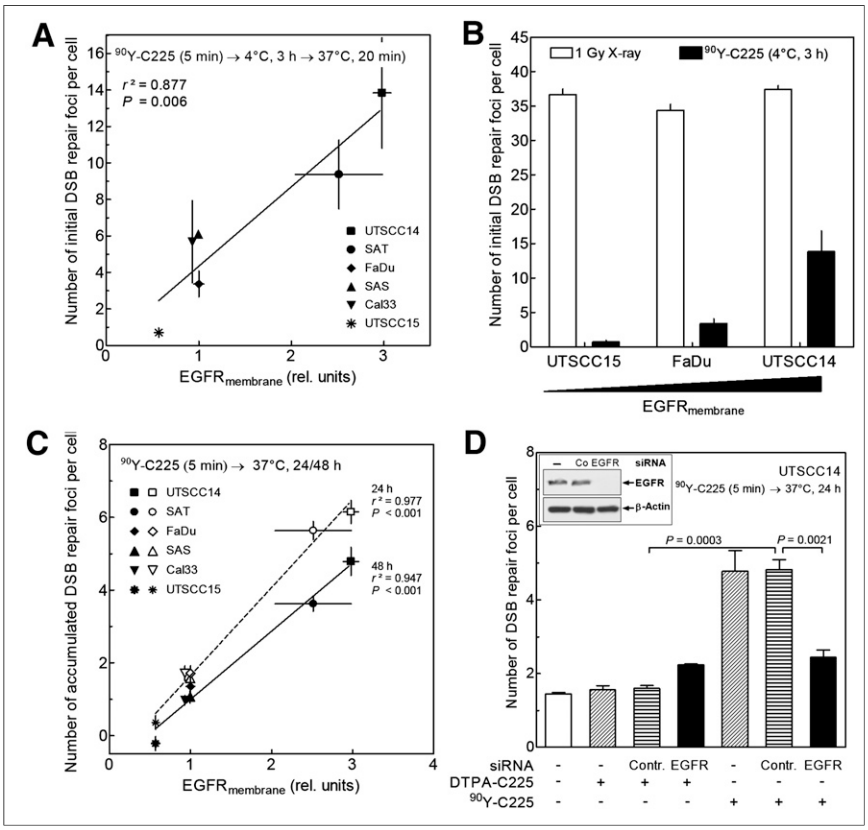

FIGURE 3. Variation in induction and accumulation of DSBs in HNSCC cell lines differing in amount of membranous EGFR. DSBs were detected by immunofluorescence staining of γH2AX/53BP1 foci. (A) Induction of DSBs through exposure to ^{90}Y-Y-CHX-A″-DTPA-cetuximab. Cells were exposed to bound ^{90}Y-Y-CHX-A″-DTPA-cetuximab for 3 h at 4°C, followed by incubation at 37°C for 20 min to allow for focus formation. Number of DSBs scored was correlated with expression of membranous EGFR as determined by Western blot analysis. (B) Induction of DSBs by 1 Gy of x-irradiation. After irradiation, cells were incubated at 37°C for 20 min to allow for focus formation. Data were taken from A for comparison with ^{90}Y-Y-CHX-A″-DTPA-cetuximab. (C) Accumulation of DSBs. Cells were exposed to bound ^{90}Y-Y-CHX-A″-DTPA-cetuximab at 37°C for 24 or 48 h, followed by detection of DSB repair foci. (D) Effect of EGFR knockdown on DSB accumulation in UTSCC14 cells. Cells were treated with siRNA for 48 h as indicated. Western blot using anti-EGFR and antiactin antibody as loading control appears in the inset. Thereafter, cells were treated with ^{90}Y-Y-CHX-A″-DTPA-cetuximab at 37°C for 24 h before analysis of DSB. Data from A and C were analyzed by linear regression.

DTPA-cetuximab at 37°C for 24 h, there was again a substantial number of remaining DSB repair foci (Fig. 3D, fifth column). This number was slightly less than the number plotted in Figure 3C, because for this experiment the specific activity of ^{90}Y-Y-CHX-A″-DTPA-cetuximab was only 60% of that used previously. However, most important, when EGFR was downregulated in UTSCC14 cells by siRNA, the number of DSB repair foci remaining was identical to the number measured for nonlabeled cells (Fig. 3D, fourth vs. seventh columns). It can also be seen that incubation with bound nonradioactive DTPA-cetuximab did not induce DSB repair foci (Fig. 3D, first and second columns). The respective immunofluorescence images are shown in Supplemental Figure 4. These results clearly demonstrate that DSB repair foci measured when cells were exposed to ^{90}Y-Y-CHX-A″-DTPA-cetuximab were due to its binding to EGFR.

Cell Killing

We next determined the effect of ^{90}Y-Y-CHX-A″-DTPA-cetuximab on cell killing. Similar to the method described above, HNSCC cell lines were allowed to bind ^{90}Y-Y-CHX-A″-DTPA-cetuximab for 5 min, followed by incubation at 37°C for 48 h before being trypsinized and seeded for colony assay. Survival was significantly correlated with the number of DSB repair foci remaining after 48 h (Fig. 4A; $r^2 = 0.989$, $P < 0.001$). UTSCC14 cells with a large number of remaining DSB repair foci also showed a strong decrease in cell survival. In contrast, the survival measured in UTSCC15 cells with nearly no remaining DSBs after exposure to ^{90}Y-Y-CHX-A″-DTPA-cetuximab was identical to the value determined after treatment with nonradioactive cetuximab.

When the surviving fraction was plotted against the respective EGFR membrane fraction, a significant correlation between these 2 parameters could also be observed

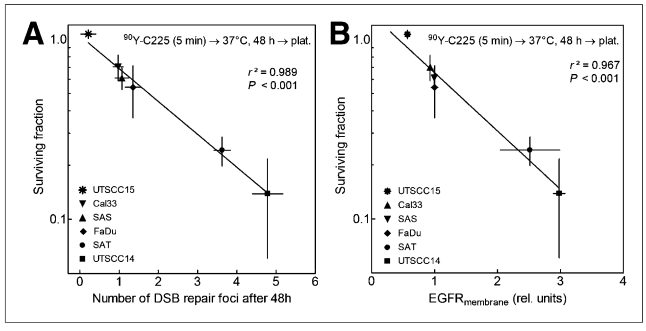

FIGURE 4. Effect of ^{90}Y-Y-CHX-A″-DTPA-cetuximab on survival of HNSCC cells differing in membranous EGFR expression. (A) Correlation between cell survival and accumulated DSBs. Cells were exposed to bound ^{90}Y-Y-CHX-A″-DTPA-cetuximab at 37°C for 48 h and then plated for cell survival. Numbers of accumulated DSBs were taken from Figure 3C. (B) Correlation between cell survival and membranous EGFR expression. EGFR expression was determined by Western blot analysis. Cell survival was determined by colony-forming assay, whereby nonlabeled CHX-A″-DTPA-cetuximab–treated cells were used as control.

(Fig. 4B; $r^2 = 0.967$, $P < 0.001$). This finding was expected, as the data in Figure 3C demonstrate that the number of remaining DSBs strongly depended on the amount of membranous EGFR. Overall, these data clearly indicate that efficient cell killing can be achieved by ^{90}Y-Y-CHX-A″-DTPA-cetuximab and that the extent of cell killing depends primarily on the amount of membranous EGFR, representing the binding sites for ^{90}Y-Y-CHX-A″-DTPA-cetuximab.

DISCUSSION

The aim of this study was to determine the extent to which radioimmunotherapy of HNSCC cells using ^{90}Y-labeled cetuximab depends on the induction and repair of DNA DSBs.

We observed that the amount of nonlabeled cetuximab that bound to the cells correlated strongly with the amount of EGFR present in the cell membrane (Fig. 1). A similar correlation and identical binding capacity are expected for labeled cetuximab, since there is no difference in binding affinity between cetuximab and DTPA-cetuximab at the oversaturated concentration applied here (Supplemental Fig. 3).

The exposure of UTSCC14 and UTSCC15 cells to bound ^{90}Y-Y-CHX-A″-DTPA-cetuximab clearly induced DSBs (Figs. 2A and 2B). These DSBs were induced by the β-particles (maximal energy = 2.28 MeV) emitted by the ^{90}Y-Y-CHX-A″-DTPA-cetuximab bound either to this cell or to one of the surrounding cells, since the mean range of these β-rays in tissue/water is about 4 mm. For the first 3 h of exposure, DSB induction occurred at a constant rate of 4.6 DSBs per hour (Fig. 2B). However, for longer exposure intervals, the rate of DSB induction is expected to decline exponentially with the known half-life of ^{90}Y (64 h) (*20*).

The initial rate of DSB induction strictly depended on the amount of membranous EGFR (Fig. 3A). That the induced DNA damage in fact specifically resulted from binding of ^{90}Y-Y-CHX-A″-DTPA-cetuximab to EGFR was demonstrated via siRNA downregulation of EGFR (Fig. 3D). Overall, the rate of DSB induction varied by a factor of 20. This finding strongly indicates that exposure to ^{90}Y-Y-CHX-A″-DTPA-cetuximab facilitates the differential targeting of HNSCC cells depending on their expression of EGFR (Fig. 3A). So far, such a differentiation has not been possible with conventional external radiotherapy.

We also measured the number of DSBs accumulated in HNSCC cells after being exposed to bound ^{90}Y-Y-CHX-A″-DTPA-cetuximab for 24 or 48 h at 37°C (Fig. 3C). These numbers represent both nonrepairable DSBs and DSBs that were recently induced but could still be rejoined. The number of DSBs measured after incubation at 37°C for 48 h was slightly less than that measured after 24 h, mostly because ^{90}Y activity decreases as the decay of ^{90}Y continues. Thus, during the first 24 h of exposure, more DSBs are induced than during the later 24-h incubation.

For the 6 HNSCC cell lines, the numbers of DSBs that had accumulated after either 24 or 48 h strictly depended on the amount of membranous EGFR and, with it, the amount of bound ^{90}Y-Y-CHX-A″-DTPA-cetuximab (Fig. 3C). These HNSCC cell lines are characterized by clear differences in DSB repair capacity (Supplemental Fig. 5). However, on exposure to bound ^{90}Y-Y-CHX-A″-DTPA-cetuximab at 37°C for 24 or 48 h, these differences in DSB repair capacity appear to have no impact on the number of accumulated DSBs. This number is determined primarily by the amount of bound ^{90}Y-Y-CHX-A″-DTPA-cetuximab and, with it, by the number of DSBs induced.

It has been previously demonstrated that blockade of EGFR by cetuximab can inhibit the repair of x-ray–induced DSBs (*18,21*). Such an inhibition is also expected when EGFR is blocked by radiolabeled cetuximab. However, the data presented here do not allow a definitive conclusion on the extent of this effect, because the numbers of DSBs that have accumulated after 24 or 48 h are determined primarily by the number of DSBs induced, whereas differences in DSB repair capacity appear to have only a minor or even negligible effect.

Exposure to bound ^{90}Y-Y-CHX-A″-DTPA-cetuximab had a clear effect on cell survival, whereby the extent of cell killing strongly correlated with the number of DSBs that had accumulated after 48 h and, with it, the amount of membranous EGFR (Figs. 4A and B). There was no cell killing in cells with low EGFR expression, but there was substantial inactivation when EGFR was strongly overexpressed. This correlation suggests that cell killing results predominantly from the DSBs induced by the 2.28-MeV β-rays emitted from bound ^{90}Y-Y-CHX-A″-DTPA-cetuximab. The greater the amount of membranous EGFR per cell, the greater is the concentration of bound ^{90}Y-Y-CHX-A″-DTPA-cetuximab and the number of DSBs induced. As a consequence, a greater number of DSBs accumulates, causing more cell inactivation. Such a straight correlation between cell survival and accumulated DSB repair foci was also seen by Cai et al. (*22*) when breast cancer cells were targeted by the radiolabeled ligand EGF using ^{111}In.

Only a few cells showed pan-nuclear staining of γH2AX for incubation at 37°C for both 24 and 48 h (Supplemental Fig. 6). Such staining is generally taken as an indication of apoptosis (*23*). There was also no sign of apoptosis when poly(adenosine diphosphate ribose)polymerase cleavage was used as an indicator of apoptosis (Supplemental Fig. 7). Therefore, we can conclude that apoptosis appears to be of minor importance for the inactivation seen here in cell cultures exposed to ^{90}Y-Y-CHX-A″-DTPA-cetuximab. In contrast, the impact of apoptosis was clearly evident when xenografts were exposed to ^{90}Y-labeled EGFR-directed mAb (*8*).

The prospect that radioimmunotherapy based on ^{90}Y-Y-CHX-A″-DTPA-cetuximab will be applied in clinics for the treatment of tumors ultimately depends on its ability to fulfill

2 main criteria: having an efficient and quantifiable effect on cell killing in tumors and having no or only modest effects on the surrounding normal tissue. The data presented here indicate that both goals appear to be achieved when ^{90}Y-Y-CHX-A″-DTPA-cetuximab is used for radioimmunotherapy. Even for cell lines with moderately enhanced EGFR expression such as Cal33, SAS, or FaDu, a substantial reduction in cell survival could be observed after exposure to bound ^{90}Y-Y-CHX-A″-DTPA-cetuximab (Fig. 4A). In contrast, for cells with a low level of EGFR such as UTSCC15—a level similar to that seen for normal fibroblasts (*2*)—no cell killing was seen on exposure to ^{90}Y-Y-CHX-A″-DTPA-cetuximab.

The data presented here for cell cultures demonstrate that the effect of ^{90}Y-Y-CHX-A″-DTPA-cetuximab on cell killing depends primarily on the amount of membranous EGFR and, as a consequence, can be quantified when this parameter is known. Therefore, when this approach is applied in the clinic, all efforts should be put toward achieving a maximal concentration of bound ^{90}Y-Y-CHX-A″-DTPA-cetuximab in the tumor. Data available so far indicate that this concentration depends on the level of tumor EGFR expression, as found here for cell cultures, but in tumors also on the specific vascularization and the chelator used (*8–10,13,14*). Therefore, the clinical application of EGFR-directed radioimmunotherapy demands a specific parameter or technique allowing monitoring of the actual concentration of the labeled mAb within the tumor.

There are several studies suggesting that PET might be the optimal tool (*9,10,24*). This technique, however, entails the combined application of a pair of isotopes such as the diagnostic β^+-emitting radionuclide ^{86}Y and the therapeutic β^--emitting radionuclide ^{90}Y, both immobilized by the same mAb to be performed in 2 consecutive procedures: a diagnostic investigation with PET before the actual treatment.

Other noninvasive techniques can likely be developed for this purpose. If one knows the actual concentration of EGFR in the tumor, the expected treatment effect can easily be quantified. In contrast to external-beam radiotherapy, such quantification does not depend on individual DSB repair capacity, the most critical parameter for cellular radiosensitivity in external radiotherapy (*15,16*).

When tumor cells with low levels of EGFR expression were exposed to bound ^{90}Y-Y-CHX-A″-DTPA-cetuximab, there was only a modest induction of DSBs, with no DSB accumulation after 48 h and hence no cell killing (Figs. 3 and 4). These data demonstrate that treatment with ^{90}Y-Y-CHX-A″-DTPA-cetuximab may theoretically also allow the optimal protection of normal tissues, since they are generally characterized by low EGFR expression (*2*). However, because ^{90}Y has a mean range of 4.3 mm, substantial cell killing would also occur on the edges of normal tissues directly adjacent to the targeted tumor cells. Therefore, other radionuclides such as ^{177}Lu with a shorter mean range of 0.28 mm (*20*) need to be tested with respect to normal-tissue protection, particularly for EGFR-directed radioimmunotherapy used to treat metastases with a diameter of 1 mm or less.

CONCLUSION

For HNSCC cells, ^{90}Y-Y-CHX-A″-DTPA-cetuximab can be used for efficient and highly specific radioimmunotherapy in vitro. This treatment brings about cell killing primarily through the induction of DNA DSBs: the higher the level of EGFR expression, the greater is the amount of ^{90}Y-Y-CHX-A″-DTPA-cetuximab bound to the cell, the number of DSBs induced, and—as a consequence—the number of cells inactivated. Further investigations are ongoing to translate these findings into in vivo models that can explore the added value that would be gained through integration of the radioimmunotherapy approach into the current standard of treatment for these tumors, that is, radiotherapy or radiochemotherapy.

DISCLOSURE

The costs of publication of this article were defrayed in part by the payment of page charges. Therefore, and solely to indicate this fact, this article is hereby marked "advertisement" in accordance with 18 USC section 1734. This research was supported by grant 02NUK006 from the German Bundesministerium für Bildung und Forschung, which is part of the German consortium on tumor targeting by radiolabeled EGFR-directed antibodies. This project was initiated by the German "Kompetenzverbund Strahlenforschung" (KVSF). The project was also supported by grant DFG (PAK-190) and in part by grant Di457/8-1 from the Deutsche Forschungsgemeinschaft. No other potential conflict of interest relevant to this article was reported.

REFERENCES

1. Bucci B, D'Agnano I, Botti C, et al. EGF-R expression in ductal breast cancer: proliferation and prognostic implications. *Anticancer Res.* 1997;17:769–774.
2. Kasten-Pisula U, Saker J, Eicheler W, et al. Cellular and tumor radiosensitivity is correlated to epidermal growth factor receptor protein expression level in tumors without egfr amplification. *Int J Radiat Oncol Biol Phys.* 2011;80:1181–1188.
3. Ang KK, Berkey BA, Tu X, et al. Impact of epidermal growth factor receptor expression on survival and pattern of relapse in patients with advanced head and neck carcinoma. *Cancer Res.* 2002;62:7350–7356.
4. Baumann M, Krause M. Targeting the epidermal growth factor receptor in radiotherapy: radiobiological mechanisms, preclinical and clinical results. *Radiother Oncol.* 2004;72:257–266.
5. Eke I, Cordes N. Dual targeting of EGFR and focal adhesion kinase in 3D grown HNSCC cell cultures. *Radiother Oncol.* 2011;99:279–286.
6. Bonner JA, Harari PM, Giralt J, et al. Radiotherapy plus cetuximab for locoregionally advanced head and neck cancer: 5-year survival data from a phase 3 randomised trial, and relation between cetuximab-induced rash and survival. *Lancet Oncol.* 2010;11:21–28.
7. Gurtner K, Deuse Y, Butof R, et al. Diverse effects of combined radiotherapy and EGFR inhibition with antibodies or TK inhibitors on local tumour control and correlation with EGFR gene expression. *Radiother Oncol.* 2011;99:323–330.

8. Liu Z, Liu Y, Jia B, et al. Epidermal growth factor receptor-targeted radioimmunotherapy of human head and neck cancer xenografts using ^{90}Y-labeled fully human antibody panitumumab. *Mol Cancer Ther.* 2010;9:2297–2308.
9. Niu G, Li Z, Xie J, Le QT, Chen X. PET of EGFR antibody distribution in head and neck squamous cell carcinoma models. *J Nucl Med.* 2009;50:1116–1123.
10. Perk LR, Visser GW, Vosjan MJ, et al. ^{89}Zr as a PET surrogate radioisotope for scouting biodistribution of the therapeutic radiometals ^{90}Y and ^{177}Lu in tumor-bearing nude mice after coupling to the internalizing antibody cetuximab. *J Nucl Med.* 2005;46:1898–1906.
11. Pfost B, Seidl C, Autenrieth M, et al. Intravesical alpha-radioimmunotherapy with ^{213}Bi-anti-EGFR-mAb defeats human bladder carcinoma in xenografted nude mice. *J Nucl Med.* 2009;50:1700–1708.
12. Ping Li W, Meyer LA, Capretto DA, Sherman CD, Anderson CJ. Receptor-binding, biodistribution, and metabolism studies of ^{64}Cu-DOTA-cetuximab, a PET-imaging agent for epidermal growth-factor receptor-positive tumors. *Cancer Biother Radiopharm.* 2008;23:158–171.
13. Wen X, Wu QP, Ke S, et al. Conjugation with ^{111}In-DTPA-poly(ethylene glycol) improves imaging of anti-EGF receptor antibody C225. *J Nucl Med.* 2001;42:1530–1537.
14. Aerts HJ, Dubois L, Perk L, et al. Disparity between in vivo EGFR expression and ^{89}Zr-labeled cetuximab uptake assessed with PET. *J Nucl Med.* 2009;50:123–131.
15. Dikomey E, Brammer I. Relationship between cellular radiosensitivity and non-repaired double-strand breaks studied for different growth states, dose rates and plating conditions in a normal human fibroblast line. *Int J Radiat Biol.* 2000;76:773–781.
16. Kasten-Pisula U, Tastan H, Dikomey E. Huge differences in cellular radiosensitivity due to only very small variations in double-strand break repair capacity. *Int J Radiat Biol.* 2005;81:409–419.
17. Diaz A, Suarez E, Blanco R, et al. Functional expression of human-epidermal-growth-factor receptor in a melanoma cell line. *Biotechnol Appl Biochem.* 2007;48:21–27.
18. Kriegs M, Kasten-Pisula U, Rieckmann T, Holst K, Dahm-Daphi J, Dikomey E. The epidermal growth factor receptor modulates DNA double strand break repair by regulating non-homologous end joining. *DNA Repair (Amst).* 2010;9:889–897.
19. Kawamoto T, Sato JD, Le A, Polikoff J, Sato GH, Mendelsohn J. Growth stimulation of A431 cells by epidermal growth factor: identification of high-affinity receptors for epidermal growth factor by an anti-receptor monoclonal antibody. *Proc Natl Acad Sci U S A.* 1983;80:1337–1341.
20. Milenic DE, Brady ED, Brechbiel MW. Antibody-targeted radiation cancer therapy. *Nat Rev Drug Discov.* 2004;3:488–499.
21. Dittmann K, Mayer C, Rodemann HP. Inhibition of radiation-induced EGFR nuclear import by C225 (cetuximab) suppresses DNA-PK activity. *Radiother Oncol.* 2005;76:157–161.
22. Cai Z, Chen Z, Bailey KE, Scollard DA, Reilly RM, Vallis KA. Relationship between induction of phosphorylated H2AX and survival in breast cancer cells exposed to ^{111}In-DTPA-hEGF. *J Nucl Med.* 2008;49:1353–1361.
23. Lu C, Zhu F, Cho YY, et al. Cell apoptosis: requirement of H2AX in DNA ladder formation, but not for the activation of caspase-3. *Mol Cell.* 2006;23:121–132.
24. Torres LA, Perera A, Batista JF, et al. Phase I/II clinical trial of the humanized anti-EGF-r monoclonal antibody h-R3 labelled with ^{99m}Tc in patients with tumour of epithelial origin. *Nucl Med Commun.* 2005;26:1049–1057.